

# Photovoltaic cooling techniques' effect on the average monthly performance

Antonino Rollo<sup>1</sup>, Vittorio Ferraro<sup>1</sup>, Piero Bevilacqua<sup>1</sup>

<sup>1</sup> Department of Mechanical, Energy and Management Engineering, University of Calabria, Rende (CS), Italy

## ABSTRACT

Nowadays, mitigating climate-altering emissions resulting from air conditioning and mechanical ventilation of indoor spaces is of utmost importance. Encourage the adoption of renewable energy sources for power generation is a critical approach in this regard. Among the available technologies, photovoltaic technology stands as the most mature option. However, it does have limitations, such as reduced efficiency and performance degradation at elevated temperatures. To enhance the efficiency of photovoltaic systems, various solutions have been proposed over time, with significant research focusing on the exploration of new materials. One of the most promising solutions involves panel cooling through the utilization of external fluids, either in a forced or natural manner. Furthermore, the extracted heat from this cooling process can be effectively reused in other industrial processes, adding to its appeal. Nonetheless, despite its potential, the application of panel cooling technology is relatively recent, and assessing its suitability in specific scenarios at an early stage can be challenging. Currently, there is a lack of clear and straightforward methodologies to evaluate the performance gains achievable through the implementation of panel cooling. The primary objective of this research is to present an innovative methodology that can effectively assess panel cooling efficiency on an average daily-monthly basis. Specifically, we propose corrective parameters that modify the widely used Siegel method, which determines the monthly average daily efficiency of uncooled panels. Throughout the study, it has become evident that the input values derived from the UNI standard do not fully represent the real-world conditions. This finding may indicate the necessity for regulatory updates to accurately account for the practical operational environment.

**Section:** RESEARCH PAPER

**Keywords:** PV cooling; experimental analysis; PV efficiency improvement; water cooling; spray cooling

**Citation:** A. Rollo, V. Ferraro, P. Bevilacqua, Photovoltaic cooling techniques' effect on the average monthly performance, Acta IMEKO, vol. 13 (2024) no. 1, pp. 1-9. DOI: [10.21014/actaimeko.v13i1.1660](https://doi.org/10.21014/actaimeko.v13i1.1660)

**Section Editor:** Francesco Lamonaca, University of Calabria, Italy

**Received** August 29, 2023; **In final form** February 5, 2024; **Published** March 2024

**Copyright:** This is an open-access article distributed under the terms of the Creative Commons Attribution 3.0 License, which permits unrestricted use, distribution, and reproduction in any medium, provided the original author and source are credited.

**Corresponding author:** Vittorio Ferraro, e-mail: [vittorio.ferraro@unical.it](mailto:vittorio.ferraro@unical.it)

## 1. INTRODUCTION

In recent years, there has been a notable global increase in electricity consumption, with a rise of approximately 1377 TW h observed from 2020 to 2021 [1]. This surge in electricity usage has particularly affected the industrial and domestic sectors. Notably, the domestic sector witnessed a spike in electricity consumption following the pandemic, driven by altered habits due to increased remote work practices ("smart working") and stay-at-home mandates [1], [2]. This trend has persisted and intensified, partly influenced by the growing adoption of electricity for final consumption [1]. Encouraging the electrification of final consumption has been a priority to replace other energy sources, like gas [3]-[5], and has led to a higher presence of household appliances and electrical conditioning systems [1]. Additionally, a shift towards more energy-intensive

lifestyles has contributed to the overall increase in electricity demand. According to the latest report by the IEA for 2022, it is projected that electricity consumption in the domestic sector will grow by 2777.78 TW h by 2030 [1].

The escalating electricity demand is linked to increasing climate-changing emissions. Consequently, meeting international agreements will require further lifestyle changes and decarbonization of the electricity system in the upcoming years. This entails promoting renewable energy sources and decentralizing electricity production. To this end, the construction of Nearly Zero Energy Building (NZEB) structures [6]-[9], which rely on renewable energy to meet their energy needs and avoid fossil fuel consumption, is being encouraged. For NZEBs, controlling thermo-hygrometric conditions and maintaining healthy indoor environments is essential. However, the systems employed for these purposes must be powered by

renewable sources to reduce climate-changing emissions [6]. To maximize the use of renewable energy systems in buildings, continued research and development of increasingly efficient systems are crucial [10], [11].

Furthermore, the current socio-economic situation, linked to the conflict in Ukraine, has contributed to a surge in energy prices, prompting the adoption of localized production plants to reduce dependency on the grid [12], [13]. This situation has facilitated the proliferation of locally located electricity production systems [14]. Among these, photovoltaic technology stands as the most mature option. However, photovoltaic systems are susceptible to climatic conditions, with performance declining as temperatures rise [1]. Over the years, efforts have been made to enhance photovoltaic systems by optimizing cell materials and exploring various cooling technologies to improve performance [15]-[19]. Passive cooling systems utilizing solid materials with high thermal conductivity, like copper or aluminium, and shaped modules to enhance heat transfer have been proposed [20]-[22]. Additionally, integrating phase change materials (PCM) into photovoltaic modules has been explored as a more complex cooling solution to reduce surface temperatures [23]-[25].

On the other hand, the functioning of active cooling systems presupposes the use of an external power, and the effectiveness must be evaluated by carrying out an overall balance between energy input and output. It must therefore be verified whether the use of an auxiliary power produces an improvement in performance such as to justify the use of the cooling system itself. An example of an active cooling system is the utilization of forced air through fans. Teo et al. [26] implemented ducts to guide the airflow through a sealed structure attached to the rear surface of the panel. This approach resulted in a significant reduction in temperature, with values decreasing from 68 °C for the uncooled panel to 38 °C for the cooled panel. Moreover, the cooling intervention led to an enhancement in efficiency, increasing from 8.6 % to 12.5 %. With a similar configuration Mazón-Hernandez et al. [27] obtained a 2 % increase in efficiency and a 15 °C reduction in cell temperature. Furthermore, they demonstrated that some parameters such as air flow, air temperature and panel elevation have a high impact on performance. Nevertheless, in a majority of the experimental applications described in the literature, water is employed as the cooling fluid, mainly due to its potential for achieving greater output power gains. Various configurations for these water-based cooling systems have been explored [28]-[31]. In systems with forced circulation of water, the fluid is forced to pass inside suitable pipes. One of the advantages of this configuration is that the extracted heat can be made available for other uses. The downside of this setup is that the water pumping system and heat exchangers are often expensive and require frequent maintenance. An alternative is immersion cooling, where the entire cake is placed in water [32]. Mehrotra et al. [33] have shown that by immersing a panel to a depth of 1 cm it is possible to obtain an efficiency improvement of about 17.8 %. Rosa-Clot et al. [34] instead studied the behaviour of the panel at a depth of 4 cm and 40 cm, identifying an increase in efficiency of about 11 % at 4 cm and a reduction of efficiency of 23 % at 40 cm.

The most promising and effective solution identified is the implementation of water spraying or spray-cooling techniques [35]. In this approach, water is delivered through nozzles, carefully atomized, and sprayed onto the panel's surface in either a continuous or intermittent manner, based on specific control strategies. These spray-cooling systems enable rapid reduction of

panel temperatures and significant improvements in its overall efficiency. However, it is worth noting that such systems may incur high water consumption.

To address this concern, the application of appropriate control strategies can be beneficial. By activating the cooling process only when a critical temperature threshold is reached and limiting its operation over time, it is possible to enhance the economic viability of these systems while maintaining their efficiency benefits. Such measures could help optimize water usage and make the implementation of spray-cooling economically feasible and environmentally sustainable. Nizetic et al. [36] in their research work they tested a monocrystalline photovoltaic panel cooled by means of 20 nozzles (10 at the front and 10 at the back). The experimental setup allowed them to evaluate the benefits achievable with only rear cooling, only front cooling, or both active cooling. The latter turned out to be the most efficient system but with the greatest expenditure of water. Between the front and rear cooling, it should be noted that the former turned out to be more efficient but over time it could damage the panel by modifying its optical characteristics if properly "softened" water was not used.

Yang et al. [37] examined a closed-cycle rear spray-cooling system. This system uses a geothermal cooling system. In different configurations and as the intensity of the radiation varied, the pump consumption and the conversion efficiency were evaluated. The payback times for such a system have been estimated, but they are still high (8.7 years in the most advantageous case).

To assess the benefits of different cooling methodologies, an experimental setup was established at the Department of Mechanical, Energy, and Management Engineering of the University of Calabria. Experimental data, including cell temperature, electrical power output, and climatic parameters, were systematically collected over several years. Previous research works have already evaluated the technical feasibility of various cooling technologies [38]-[40]. However, the present study aims to leverage the extensive data collected to devise a straightforward methodology applicable at a daily-monthly level for assessing panel performance under different cooling configurations.

The proposed approach builds upon Siegel's widely used methodology in the literature for evaluating the average daily panel performance [41]. Our method entails determining the increase in performance achieved for each cooling configuration and appropriately normalizing it relative to the performance assessed under Standard Test Conditions (STC). These factors will be determined through fitting techniques applied to the abundant experimental data accumulated over the years.

The outcome will be a versatile methodology enabling the evaluation of the technical feasibility of various configurations by adjusting the efficiency based on the cooling system employed. Such methodologies can encourage the adoption of novel plant technologies, thereby reducing the reliance on non-renewable energy at the domestic level. Improved efficiency translates to enhanced productivity per unit of surface area, making these advancements in cooling systems particularly advantageous for sustainable energy production.

## 2. MATERIALS AND METHODS

### 2.1. Experimental site

At the rooftop of the 45C cube at the Department of Mechanical, Energy, and Management Engineering of the



Figure 1. Experimental plant located at the cube 45C of the Department of Mechanical, Energy and Management Engineering of the University of Calabria.

Table 1. Main characteristics of photovoltaic modules and micro-inverters.

PV Modules	
Dimensions	1.663 m × 0.998 m
Area	1.46 m <sup>2</sup>
Number of cells	60
Nominal Power in W	245
Efficiency in %	14.5
Output tolerance in %	+5 / -0
Rated voltage in V	29.9
Rated current in A	8.2
Open circuit voltage in V	37.41
Short circuit current in A	8.8
Temperature coefficient – P <sub>mpp</sub> , in %/K	-0.43
Temperature coefficient – I <sub>sc</sub> , in %/K	0.06
Temperature coefficient - U <sub>oc</sub> , in %/K	-0.31
Normal Operating Cell Temperature in °C	43 ± 2
Micro-inverter	
Maximum DC power in W	265
Operative DC input voltage in V	18 ÷ 58
MPPT DC voltage range in V	20 ÷ 50
Maximum DC input Voltage in V	65
Maximum DC input current in A	10
Start voltage DC input in V	25
Nominal outlet AC power in W	250
Nominal outlet AC voltage in V	230
AC output voltage range in V	180 ÷ 264
Maximum AC output current in A	1.2

University of Calabria (Arcavacata di Rende – CS, Italy. Latitude: 39° 21'), an experimental setup is installed (Figure 1). This setup comprises six photovoltaic panels, all possessing identical characteristics but operating under various conditions. The panels are inclined at an angle of 30 ° and are oriented to the south, ensuring optimal positioning for solar exposure. To prevent any mutual radiation or shading interference, the panels are strategically arranged in a manner that avoids such effects.

Each of the photovoltaic panels is equipped with a micro-inverter, enabling individual optimization of their operations independently from one another. In Table 1, the key characteristics of the photovoltaic panels and micro-inverters are summarized for reference.

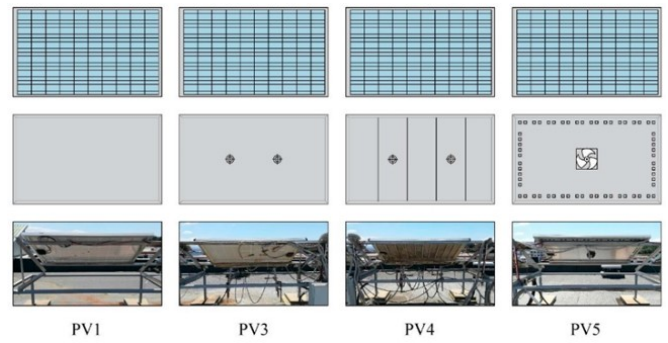


Figure 2. PV1, reference PV module without cooling; PV3, PV module with spray-cooling on the backside; PV4, PV module with spray-cooling on the backside and metallic layer in way to uniform the cooling effect; PV5, PV module with a fan and an air channel on the backside.

## 2.2. Cooling strategies

The experimental site consists of panels equipped with various cooling technologies, as illustrated in Figure 2. Specifically:

- PV1: This panel serves as the reference for performance analysis and does not have any cooling systems in place.
- PV3: This panel is cooled using rear spray-cooling. It features two nozzles located 50cm away from the rear surface. These nozzles operate at a pressure of 3 bar and have a nominal flow rate of 8.55 l/min. The nozzles are directly connected to the water mains, and the spray-cooling is activated when the rear panel temperature reaches 40 °C, maintained for 5 seconds.
- PV4: Similar to PV3, this panel is equipped with rear spray-cooling, but with an additional thin metal layer on the rear face to homogenize the cooling effect.
- PV5: This panel is cooled by an electric fan. A closed metal structure has been created on the rear face, with the fan centrally positioned to draw air that recirculates through holes on the structure's perimeter. In this case, the fan operates continuously throughout the day.

## 2.3. Data acquisition systems

An adjacent meteorological station has been installed near the experimental site to facilitate the collection of various climatic parameters. This station enables the acquisition of data such as air temperature, relative humidity, wind speed, and solar radiation. The sensor specifications are summarized in Table 2. Solar radiation is evaluated on the plane of the panels (at an inclination of 30 °).

For every panel, measurements of rear temperature, output voltage, and current (on the alternating current side) are recorded. Table 3 provides an overview of the sensors installed

Table 2. Sensor specifications of the climatic station.

Parameter	Sensor	Pt 100 1/3
	Temperature	Range in °C
Accuracy in °C		± 0.1
Relative Humidity	Sensor	Capacitive
	Range in %	0 ÷ 100
Wind Speed	Accuracy in %	± 1.5 (RH5 - 95%)
	Sensor	ANEMOMETER
Solar irradiance	Range in m/s	0 ÷ 75
	Sensor	PYRANOMETER
	Range in nm	295 ÷ 2800

Table 3. Sensor specifications for each photovoltaic panel.

Temperature	Sensor	Pt 100 1/3
	Range in °C	-50 ÷ 70
	Accuracy in K	± 0.1
Current	Sensor	DC SHUNT
	Range in A	5 ÷ 1200
	Rated Accuracy in %	± 0.25
Voltage	Sensor	DSCA31-15
	Range in V	0 ÷ 40
	Accuracy in %	± 0.03

on each individual panel. The rear temperatures are acquired at four distinct points on the rear face of each panel, arranged along the diagonal. It is important to note that the values utilized in this research represent average values, specifically daily monthly averages.

The voltage ( $V$ ), current ( $I$ ) and incident frontal radiation ( $G$ ) were used to determine the electric power produced ( $P_{el}$ ) and the efficiency ( $\eta$ ) of the experimental panel by the following equations.

$$P_{el} = V \cdot I \quad (1)$$

$$\eta = \frac{P_{el}}{A \cdot G}, \quad (2)$$

where  $A$  represents the area of the photovoltaic module.

Experimental data were collected over several years from 2017 to 2019, with a sampling time of 60 seconds, subsequently these were averaged at a monthly average daily level.

To obtain the monthly average daily values, Equation (3) was employed.

$$\bar{\eta}_{gmm} = \frac{\sum_i^N P_{el,i}}{A \cdot \frac{\sum_i^N G_i}{N}}, \quad (3)$$

where  $N$  denotes the number of data points measured in the respective month.

By comparing the experimental data with simulated data using the Siegel method, the objective was to verify that the proposed methodology yields excellent results even under reference conditions. Subsequently, to apply the Siegel method to the cooled configurations, corrective coefficients were obtained through fitting methodologies, which will be elaborated further in the subsequent paragraph.

#### 2.4. Evaluation of the simulated energy production (Siegel methodology)

The monthly daily average electricity (m.d.a.) supplied by a photovoltaic panel can be determined using Equation (4).

$$\bar{E}_e = A \cdot \bar{E} \cdot \bar{\eta}, \quad (4)$$

where  $\bar{E}$  is the monthly average daily solar energy incident on 1 m<sup>2</sup> of panel and  $\bar{\eta}$  is the monthly average daily efficiency. This latter is calculated by means of Equation (5).

$$\bar{\eta}_{Siegel} = \eta_R \cdot \left[ 1 - \beta \cdot (\bar{T}_a - T_R) - \frac{\beta \cdot (\bar{\tau}\bar{\alpha}) \cdot V \cdot \bar{E}}{n \cdot U_c} \right], \quad (5)$$

where  $\eta_R$  is the reference efficiency in the STC (standard test conditions),  $\beta$  is the power temperature coefficient (%/K),  $\bar{T}_a$  is the monthly average air temperature,  $T_R$  is the reference

temperature,  $\bar{\tau}\bar{\alpha}$  is the monthly average value of the product  $\bar{\tau}\bar{\alpha}$  and  $V$  is a dimensionless variable that can be calculated with Equation (6)

$$V = a \cdot X^2 + b \cdot X + c, \quad (6)$$

where  $X$ ,  $a$ ,  $b$  and  $c$  are parameters whose expressions are referred to in specific texts [41]. These parameters are expressed as a function of the following quantities:

- $\bar{R}$ , i.e. the global inclination factor of the daily mean monthly radiation.
- $R_n$ , which is the ratio between the hourly radiation incident at noon on the plane of the panels and that incident at noon on the horizontal plane, for the average monthly day.
- $\bar{K}$ , which is the average monthly serenity index.
- $h_a$ , which is the hour angle of sunrise.
- $h_a'$ , which is the hour angle of sunrise on the surface of the panels.

The monthly average daily external air temperature values and the monthly average daily incident radiation on the inclined plane for the examined location (Cosenza) are obtained using the UNI 10349 standard [42].

#### 2.5. Innovative formulation of the increase factor of the efficiency (methodology)

To determine the corrective factors for the performance assessed using the methodology described earlier, the external air temperature (in °C), incident solar radiation on the inclined plane (in MJ/m<sup>2</sup>), and electric power produced under various configurations (in W) were calculated at a monthly daily average level. This allowed the calculation of the average monthly daily efficiency for each individual configuration using Equation (3).

Next, the differences in efficiency were calculated concerning the efficiency obtained with the Siegel method at the monthly daily average level ( $\bar{\eta}_{Siegel,i}$ ), where  $i$  denotes the  $i$ -th month considered. Linear regressions were performed on the experimental data using fitting procedures. Consequently, for each configuration, the differences in experimental efficiency ( $\bar{\eta}_{PV,exp,i}$ ) compared to the efficiency calculated with the Siegel method ( $\bar{\eta}_{Siegel,i}$ ) were determined at the average monthly daily level, suitably normalized with respect to the efficiency in the STC (Standard Test Conditions):

$$\Delta\bar{\eta}_{PV1,exp,i} = \frac{\bar{\eta}_{PV1,exp,i} - \bar{\eta}_{Siegel,i}}{\eta_{STC}} \quad (7)$$

$$\Delta\bar{\eta}_{PV3,exp,i} = \frac{\bar{\eta}_{PV3,exp,i} - \bar{\eta}_{Siegel,i}}{\eta_{STC}} \quad (8)$$

$$\Delta\bar{\eta}_{PV4,exp,i} = \frac{\bar{\eta}_{PV4,exp,i} - \bar{\eta}_{Siegel,i}}{\eta_{STC}} \quad (9)$$

$$\Delta\bar{\eta}_{PV5,exp,i} = \frac{\bar{\eta}_{PV5,exp,i} - \bar{\eta}_{Siegel,i}}{\eta_{STC}}. \quad (10)$$

The experimental data were subjected to fitting procedures using optimization techniques with respect to two parameters: the monthly daily average external air temperature in the  $i$ -th month ( $\bar{T}_{a,gmm,i}$ ) and the irradiation on the inclined plane of the panels ( $\bar{G}_{gmm,i}$ ) during the same month.



### 3. RESULTS

#### 3.1. Evaluation of the experimental energy production

The hourly trends of the electric power produced by the PV1, PV3, PV4 and PV5 panels for a typical sunny winter day (December 21st), for a typical sunny summer day (June 21st) and for a typical cloudy day (September 14th) are shown in Figure 3, Figure 4 and Figure 5, respectively.

It is observed that the effects of the cooling systems are perceptible only on sunny days and have no particular influence on cloudy days. Furthermore, it should be noted that among the technologies proposed, the most efficient is the one installed in the PV3 panel, i.e. the rear spray-cooling without a metal layer to uniform the cooling effect. Therefore, the addition of a further metal layer behind the panel does not allow to obtain the desired effect but it reduces the heat exchange with the external environment and the efficiency of the cooling itself. Finally, it is noted that the worst configuration is that used in the PV4 panel in which the cooling by means of mechanical ventilation and a rear air gap is not particularly efficient, especially in summer conditions. Indeed, in summer conditions it is used for cooling the warm outside air which does not produce a considerable cooling effect. Furthermore, the rear metal air gap creates a

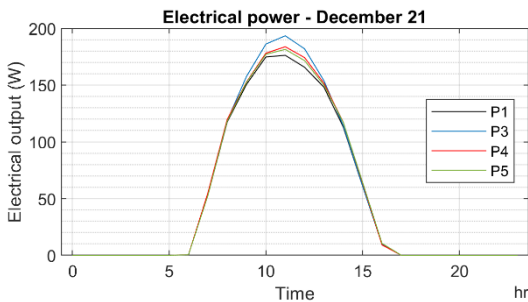


Figure 3. Electrical power distribution on the 21st of December (winter day) for the different configurations.

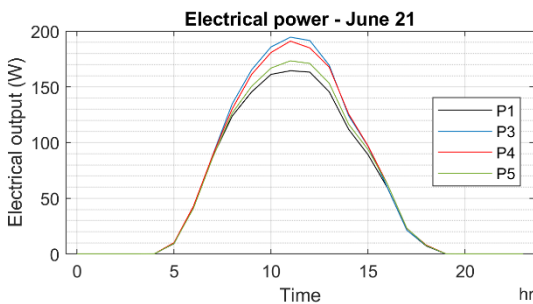


Figure 4. Electrical power distribution on the 21st of July (summer day) for the different configurations.

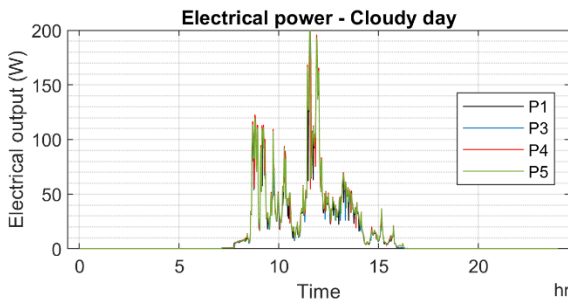


Figure 5. Electrical power distribution on the 14th of September (cloudy day) for the different configurations.

thermal accumulation with heat that comes both from the photovoltaic panel and from the surrounding environment.

It is concluded that rear spray-cooling is the most efficient methodology, and it allows obtaining benefits in terms of producibility on all sunny days regardless of the time of year.

#### 3.2. Evaluation of the simulated energy production in the reference case (results)

As described in Paragraph 2.4, it is possible to calculate the average monthly efficiency of an uncooled panel based on the location and its corresponding climatic parameters. The Siegel method was utilized for this purpose, requiring input values of the daily monthly average air temperature and solar radiation on the inclined plane. These values were obtained from the UNI 10349:2016 standard. The comparison between the data obtained using the Siegel method and the experimental values measured at the site of interest is shown in Figure 6 and Figure 7, respectively, for the external temperature and solar radiation.

The experimental values were derived by considering all the available measurement data from different years. This comparison allows for a comprehensive evaluation of the accuracy and agreement between the simulated values based on the standard data and the actual experimental results for the given location.

A systematic error is evident in both analysed parameters. Specifically, the values derived from the standard appear to be underestimated for the specific locality under examination. Consequently, this error impacts the efficiency calculated using the Siegel method when relying on input values from the legislation. The discrepancy could be attributed to the observed changes in climatic conditions over recent years, indicating a potential need for updating the values specified in the legislation.

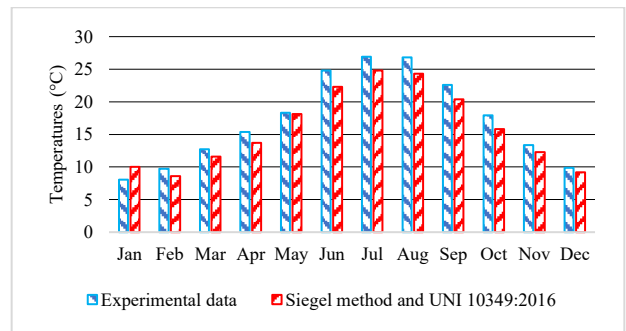


Figure 6. Comparison between the daily monthly mean temperature evaluate by means of the UNI 10349:2016 legislation and the daily monthly mean and measured temperature.

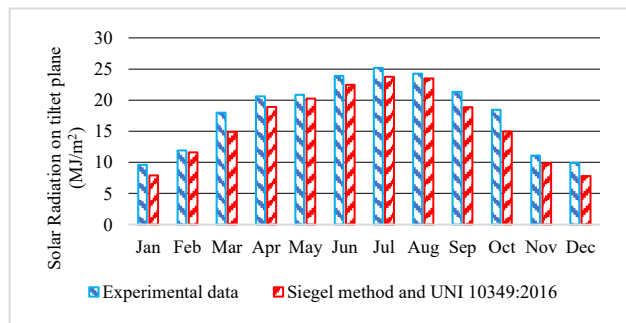


Figure 7. Comparison between the daily monthly mean irradiance evaluate by means of the UNI 10349:2016 legislation and the daily monthly mean measured irradiance.

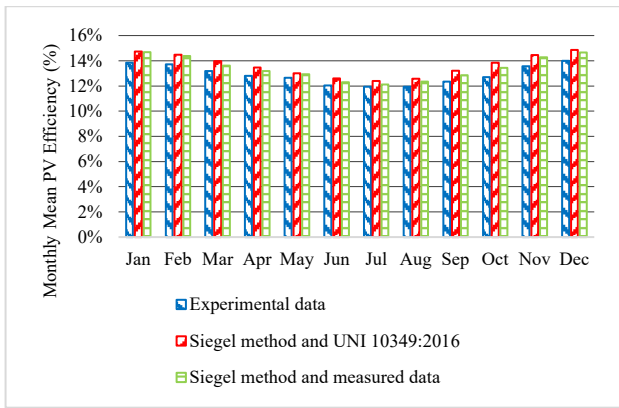


Figure 8. Comparison between the daily monthly mean efficiency evaluate by means of the Siegel methodology with UNI 10349:2016 input data, daily monthly mean efficiency evaluate by means of the Siegel methodology with measured input data and daily monthly mean measured efficiency in the reference case.

Figure 8 illustrates the comparison between the average daily and monthly trends of measured and simulated efficiency using the methodology described in Paragraph 2.4. The plot includes both the simulated trend obtained with input parameters from the national legislation and the simulated trend achieved using the measured values of external air temperature and incident solar radiation specific to the location.

It is evident that, in all months, the values simulated with the input parameters from the legislation appear to be higher compared to the experimental data. However, utilizing the measured values of external air temperature and incident solar radiation as input for the Siegel method yields efficiency values that closely align with the measured data. This effect is especially pronounced during warmer months. These results reinforce the need for possible updates to the values present in the standard to ensure accurate and reliable efficiency estimations.

### 3.3. Innovative formulation of the increase factor of the efficiency (results)

Using the procedure outlined in Section 2.5, the following linear regressions were obtained for each panel (PV1, PV3, PV4 and PV5).

$$\Delta\bar{\eta}_{PV1,mod,i} = -0.07567 - 0.00122 \cdot T_{a, gmm,i} + 0.002779 \cdot G_{gmm,i} \quad (11)$$

$$\Delta\bar{\eta}_{PV3,mod,i} = -0.094 + 0.000788 \cdot T_{a, gmm,i} + 0.004355 \cdot G_{gmm,i} \quad (12)$$

$$\Delta\bar{\eta}_{PV4,mod,i} = -0.07215 - 0.0001523 \cdot T_{a, gmm,i} + 0.003564 \cdot G_{gmm,i} \quad (13)$$

$$\Delta\bar{\eta}_{PV5,mod,i} = -0.06581 - 0.001795 \cdot T_{a, gmm,i} + 0.00363 \cdot G_{gmm,i} \quad (14)$$

It is important to note that a corrective factor was also obtained for the reference panel (PV1), which takes into account the deviation of the Siegel method concerning the experimental data. This deviation is primarily attributed to the lack of updating in the external air temperature and radiation values as specified in the legislation. These corrective parameters allow for the reduction of efficiency deviations in the various configurations

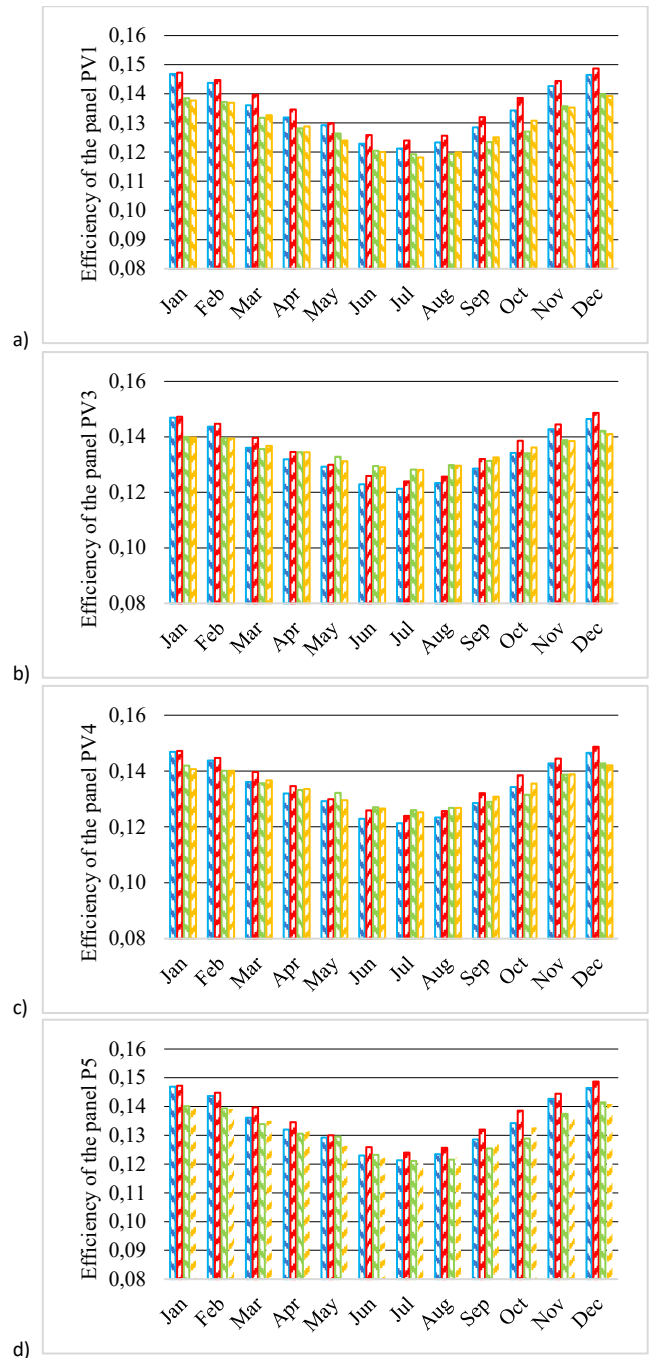


Figure 9. Comparison between the daily monthly mean efficiency evaluate by means of the Siegel methodology with UNI 10349:2016 input data, daily monthly mean efficiency evaluate by means of the Siegel methodology with measured input data, daily monthly mean measured efficiency and daily monthly mean efficiency simulated with the proposed model: a) PV1 module, b) PV3 module, c) PV4 module and d) PV5 module.

when compared to the efficiency calculated using the Siegel method in combination with the standard values of external air temperature and radiation on the inclined plane, obtained through daily average monthly measurements.

In order to demonstrate the goodness of the relationships obtained, the comparisons between the efficiency calculated using the Siegel method in combination with the values of the UNI 10349:2016 standard, the values of the efficiency calculated with the Siegel method in combination with the measured values, the efficiency obtained from the experimental data and the efficiency obtained by correcting the Siegel method (in

combination with the legislation values) with the parameters obtained from the previous regressions are shown in Figure 9.

In all cases it is observed that in most months of the year there is an excellent correspondence between the experimental values and those obtained with the methodology proposed in this research work. In order to better highlight this aspect, error indices were calculated in the following cases:

- Comparison between the values obtained through the Siegel method combined with the standard data and the experimental values.
- Comparison between the values obtained through the Siegel method combined with the measured data and the experimental values.
- Comparison between the proposed model and the experimental values.

All panels were subject to these comparisons. Specifically, the errors were analysed in terms of Root Mean Square Error (RMSE) and Root Mean Square Error Percentage (RMSEP). The relationships utilized for these calculations are presented below.

$$RMSE = \sqrt{\frac{\sum_i (a_i - e_i)^2}{d}} \quad (15)$$

$$RMSEP = \sqrt{\frac{\sum_i \left(\frac{a_i - e_i}{e_i}\right)^2}{d}}, \quad (16)$$

where  $a_i$  represents the modelled value and  $e_i$  represents the true experimental value. The results obtained from these calculations are presented in Table 4.

It is observed that in all cases the proposed model allows to obtain the best results in terms of correspondence between modelled data and experimental data.

### 3.4. Uncertainty analysis

To evaluate the possible errors made in the data measurement phase, an analysis of the uncertainty of the model was carried out. In particular, the objective is to evaluate how the uncertainty of the measuring instruments influence the evaluation of the final calculated quantity. The main quantity examined within this research work is the average daily efficiency of the photovoltaic module which is evaluated by means of Equation (3). The complication in evaluating model uncertainty is having to work with monthly average daily values.

Taking as reference a generic parameter  $P$  function of different independent variables  $x_i$ :

$$P = P(x_1; x_2; \dots; x_n). \quad (17)$$

It is possible to evaluate the uncertainty of the parameter due to uncertainty from the measures from the variables independent  $x_i$  through the following equation [43]-[46]:

$$\varepsilon_P = \sqrt{\sum_{i=1}^n \left(\frac{\partial P}{\partial x_i} \cdot \varepsilon_i\right)^2}. \quad (18)$$

In the case under examination, the independent variables that contribute to the calculation of the efficiency of the photovoltaic module are the electrical power and the frontal radiation incident on the module. The electric power is not measured directly but

Table 4. Sensor specifications for each photovoltaic panel.

	Comparison	Siegel method and UNI 10349	Siegel method and measured data	Proposed model
$\bar{\eta}_{PV1}$	RMSE	0.0076	0.0054	0.0015
	RMSEP	5.87 %	4.07 %	1.18 %
$\bar{\eta}_{PV3}$	RMSE	0.0045	0.0046	0.0010
	RMSEP	3.32 %	3.48 %	0.75 %
$\bar{\eta}_{PV4}$	RMSE	0.0042	0.0034	0.0016
	RMSEP	3.04 %	2.52 %	1.21 %
$\bar{\eta}_{PV5}$	RMSE	0.0058	0.0037	0.0017
	RMSEP	4.35 %	2.74 %	1.28 %

the voltage ( $V$ ) and the current ( $I$ ) of the DC side panel are measured (as seen in Section 2.1).

Developing this procedure for the case under examination, the following relationship is obtained:

$$\varepsilon_{\eta} = \sqrt{(\varepsilon_V^2 + \varepsilon_I^2) \cdot \frac{\sum_{j=1}^N (V_j \cdot I_j)^2}{\left(\sum_{j=1}^N V_j \cdot I_j\right)^2} + \varepsilon_G^2 \cdot \frac{\sum_{j=1}^N (G_j)^2}{\left(\sum_{j=1}^N G_j\right)^2}}, \quad (19)$$

where the uncertainties of the independent variables are summarized in Table 2 and Table 3. The one just calculated is the combined standard uncertainty and is equivalent to a *standard deviation* of a normal distribution which covers 68.7 % of the values object of the distribution itself (this is defined as the *level of confidence*). An expanded uncertainty can be defined by multiplying this uncertainty by a *coverage factor* ( $k$ ). Generally,  $k$  is set equal to 2 in such a way as to obtain a 95 % confidence level. The expanded uncertainty was calculated with  $k = 2$  for each single month considering the values measured per minute. They sum up the results obtained in the Table 5.

It is observed that for all the configurations there is an uncertainty which varies between 0.031 % and 0.045 %. These values are perfectly acceptable. To demonstrate the goodness of the results obtained, Figure 10 shows the trends of the average daily efficiencies for the various configurations with the relative error bands with a confidence interval of 95 %.

Table 5. Uncertainty values of the daily monthly mean efficiencies in the different configurations.

Months	$\varepsilon_{PV1}$	$\varepsilon_{PV3}$	$\varepsilon_{PV4}$	$\varepsilon_{PV5}$
Jan	0.0452 %	0.0452 %	0.0451 %	0.0452 %
Feb	0.0426 %	0.0426 %	0.0425 %	0.0425 %
Mar	0.0350 %	0.0350 %	0.0350 %	0.0350 %
Apr	0.0389 %	0.0389 %	0.0389 %	0.0389 %
May	0.0352 %	0.0352 %	0.0352 %	0.0352 %
Jun	0.0318 %	0.0318 %	0.0318 %	0.0318 %
Jul	0.0312 %	0.0312 %	0.0312 %	0.0312 %
Aug	0.0316 %	0.0316 %	0.0316 %	0.0316 %
Sep	0.0335 %	0.0336 %	0.0335 %	0.0335 %
Oct	0.0352 %	0.0352 %	0.0352 %	0.0352 %
Nov	0.0413 %	0.0414 %	0.0413 %	0.0413 %
Dec	0.0413 %	0.0413 %	0.0412 %	0.0412 %
Max	0.0452 %	0.0452 %	0.0451 %	0.0452 %
Min	0.0312 %	0.0312 %	0.0312 %	0.0312 %

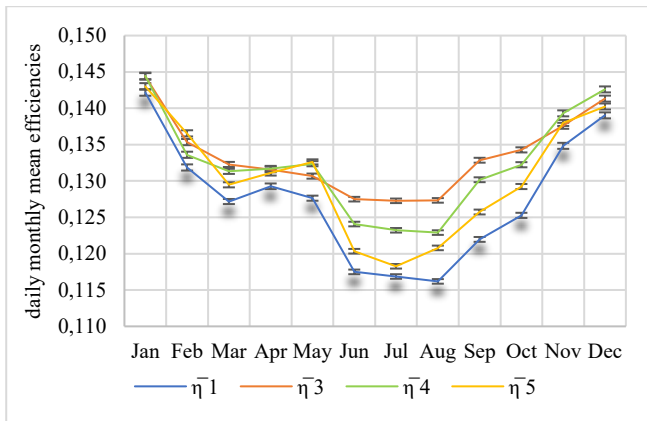


Figure 10. Comparison of the daily monthly mean measured efficiencies and their tolerance in the different configurations.

It can be observed that the error bands are very limited in each point.

#### 4. CONCLUSIONS

In the present research, the focus was on exploring new technologies that can effectively reduce the environmental impact for end users at the domestic level. To achieve this, various system configurations for photovoltaic modules serving air conditioning and ventilation systems within internal environments were analysed. Particularly, investigations were conducted on novel technologies capable of enhancing module efficiency through cooling techniques.

To assess the technical and economic viability of these cooling technologies, a methodology was introduced, enabling the determination of photovoltaic panel efficiency based on the Siegel methodology. This approach allows the evaluation of average daily efficiency, utilizing input values for external air temperature and incident radiation on the inclined panel surface, obtained from the UNI standard. However, it was observed that this methodology was inadequate for directly assessing efficiency in different cooled configurations. Moreover, a deviation was noted, indicating the potential need for updates in the temperature and radiation data specified in the legislation.

Three distinct cooling methods were considered, and for each, a corrective parameter for the Siegel model was derived through fitting procedures using experimental data. Subsequently, the Siegel method, corrected for the various cooling configurations, underwent experimental validation. The results demonstrated an excellent correlation between the experimental data and the proposed methodology, with remarkably low RMSE (Root Mean Square Error) and RMSEP (Root Mean Square Percentage Error) values across all cases. The maximum values obtained were 0.00166 and 1.28 %, respectively. Finally, an uncertainty analysis was conducted which highlighted the goodness of the experimental data used for the validation of the model.

The proposed methodology holds significant potential as a valuable tool in future design phases, particularly if cooling systems become more widely adopted. Its simplicity and ease of application make it an excellent means to assess the feasibility of this technology at an early stage. As the research progresses, potential future developments may involve evaluating energy savings and the reduction of climate-altering emissions attainable through various configurations for a reference building, even

when the building's location and aspect ratio vary. This extended analysis would provide valuable insights into the overall effectiveness and environmental impact of employing these cooling systems in diverse architectural contexts.

#### REFERENCES

- [1] IEA - International Energy Agency, Website. Online [Accessed 8 February 2023] <https://www.iea.org/>
- [2] Terna, Terna grid operator. Online [Accessed 8 February 2023] <https://www.terna.it/en>
- [3] R. Bruno, F. Nicoletti, G. Cuconati, S. Perrella, D. Cirone, Performance indexes of an air-water heat pump versus the capacity ratio: Analysis by means of experimental data, *Energies*, 13(13). DOI: [10.3390/en13133391](https://doi.org/10.3390/en13133391)
- [4] F. Nicoletti, M. A. Cucumo, N. Arcuri, Cost optimal sizing of photovoltaic-battery system and air-water heat pump in the Mediterranean area, *Energy Conversion and Management*, 270, 116274. DOI: [10.1016/j.enconman.2022.116274](https://doi.org/10.1016/j.enconman.2022.116274)
- [5] M. Cucumo, V. Ferraro, D. Kaliakatsos, M. Mele, F. Nicoletti, Calculation model using finite-difference method for energy analysis in a concentrating solar plant with linear Fresnel reflectors. *Int. Journal of Heat and Technology*, 34(Special Issue 2). DOI: [10.18280/ijht.34S221](https://doi.org/10.18280/ijht.34S221)
- [6] F. Nicoletti, M. Cucumo, N. Arcuri, Building-integrated photovoltaics (BIPV): A mathematical approach to evaluate the electrical production of solar PV blinds. *Energy*, 263, 126030. DOI: [10.1016/j.energy.2022.126030](https://doi.org/10.1016/j.energy.2022.126030)
- [7] R. Bruno, C. Carpino, P. Bevilacqua, J. Settino, N. Arcuri, A novel Stay-In-Place formwork for vertical walls in residential nZEB developed for the Mediterranean climate: hygrothermal, energy, comfort and economic analyses, *Journal of Building Engineering*, Vol. 45, January 2022, 103593. DOI: [10.1016/j.jobbe.2021.103593](https://doi.org/10.1016/j.jobbe.2021.103593)
- [8] J. Settino, C. Carpino, S. Perrella, N. Arcuri, Multi-Objective Analysis of a Fixed Solar Shading System in Different Climatic Areas, *Energies*, 13, 3249. DOI: [10.3390/en13123249](https://doi.org/10.3390/en13123249)
- [9] R. Bruno, V. Ferraro, P. Bevilacqua, J. Settino, A. Rollo, Experimental tests to assess the effects of Phase Change Materials in building envelopes. *IEEE Int. Workshop on Metrology for Living Environment (MetroLivEnv)*, Milano, Italy, pp. 168-172, DOI: [10.1109/MetroLivEnv56897.2023.10164031](https://doi.org/10.1109/MetroLivEnv56897.2023.10164031)
- [10] F. Nicoletti, D. Kaliakatsos, V. Ferraro, M. A. Cucumo, Analysis of the energy and visual performance of a building with photochromic windows for a location in southern Italy, *Building and Environment*, 224, 109570. DOI: [10.1016/j.buildenv.2022.109570](https://doi.org/10.1016/j.buildenv.2022.109570)
- [11] D. Kaliakatsos, F. Nicoletti, F. Paradisi, P. Bevilacqua, N. Arcuri, Evaluation of Building Energy Savings Achievable with an Attached Bioclimatic Greenhouse: Parametric Analysis and Solar Gain Control Techniques. *Buildings* 2022, 12, 2186. DOI: [10.3390/buildings12122186](https://doi.org/10.3390/buildings12122186)
- [12] M. A. Cucumo, V. Ferraro, D. Kaliakatsos, M. Mele, F. Nicoletti, Linear Fresnel plant with primary reflectors movable around two axes, *Advances in Modelling and Analysis A*, Vol. 55, No. 3, pp. 99-107. DOI: [10.18280/ama\\_a.550301](https://doi.org/10.18280/ama_a.550301)
- [13] M. A. Cucumo, V. Ferraro, D. Kaliakatsos, M. Mele, F. Nicoletti, Law of motion of reflectors for a linear Fresnel plant. *Int. Journal of Heat and Technology*, 35 (Special Issue 1). DOI: [10.18280/ijht.35Sp0111](https://doi.org/10.18280/ijht.35Sp0111)
- [14] M. A. Cucumo, V. Ferraro, D. Kaliakatsos, F. Nicoletti, Study of kinematic system for solar tracking of a linear Fresnel plant to reduce end losses. *European J. of Electrical Engineering*, 21(5). DOI: [10.18280/ejee.210501](https://doi.org/10.18280/ejee.210501)



- [15] E. Skoplaki, J. Palyvos, On the temperature dependence of photovoltaic module electrical performance: A review of efficiency/power correlations, *Solar Energy*, 83(5). DOI: [10.1016/j.solener.2008.10.008](https://doi.org/10.1016/j.solener.2008.10.008)
- [16] J. Day, S. Senthilarasu, T. K. Mallick, Improving spectral modification for applications in solar cells: A review, *Renewable Energy* (Vol. 132). DOI: [10.1016/j.renene.2018.07.101](https://doi.org/10.1016/j.renene.2018.07.101)
- [17] R. Bruno, P. Bevilacqua, L. Longo, N. Arcuri, Small size single-axis PV trackers: Control strategies and system layout for energy optimization, *Energy Procedia*, 82. DOI: [10.1016/j.egypro.2015.11.802](https://doi.org/10.1016/j.egypro.2015.11.802)
- [18] J. Siecker, K. Kusakana, B. P. Numbi, A review of solar photovoltaic systems cooling technologies, *Renewable and Sustainable Energy Reviews* (Vol. 79). DOI: [10.1016/j.rser.2017.05.053](https://doi.org/10.1016/j.rser.2017.05.053)
- [19] F. Nicoletti, M. A. Cucumo, V. Ferraro, D. Kaliakatsos, J. Settino, Performance analysis of a double-sided PV plant oriented with backtracking system, *Mathematical Modelling of Engineering Problems*, Vol. 7, No. 3, pp. 325-334. DOI: [10.18280/mmep.070301](https://doi.org/10.18280/mmep.070301)
- [20] M. Sharaf, M. S. Yousef, A. S. Huzayyin, Review of cooling techniques used to enhance the efficiency of photovoltaic power systems, *Environmental Science and Pollution Research* (Vol. 29, Issue 18). DOI: [10.1007/s11356-022-18719-9](https://doi.org/10.1007/s11356-022-18719-9)
- [21] H. Alizadeh, R. Ghasempour, M. B. Shafii, M. H. Ahmadi, W. M. Yan, M. A. Nazari, Numerical simulation of PV cooling by using single turn pulsating heat pipe, *Int. Journal of Heat and Mass Transfer*, 127. DOI: [10.1016/j.ijheatmasstransfer.2018.06.108](https://doi.org/10.1016/j.ijheatmasstransfer.2018.06.108)
- [22] J. G. Hernandez-Perez, J. G. Carrillo, A. Bassam, M. Flota-Banuelos, L. D. Patino-Lopez, A new passive PV heatsink design to reduce efficiency losses: A computational and experimental evaluation, *Renewable Energy*, 147. DOI: [10.1016/j.renene.2019.09.088](https://doi.org/10.1016/j.renene.2019.09.088)
- [23] T. Ma, H. Yang, Y. Zhang, L. Lu, X. Wang, Using phase change materials in photovoltaic systems for thermal regulation and electrical efficiency improvement: A review and outlook, *Renewable and Sustainable Energy Reviews* (Vol. 43). DOI: [10.1016/j.rser.2014.12.003](https://doi.org/10.1016/j.rser.2014.12.003)
- [24] A. Waqas, J. Ji, Thermal management of conventional PV panel using PCM with movable shutters – A numerical study, *Solar Energy*, 158. DOI: [10.1016/j.solener.2017.10.050](https://doi.org/10.1016/j.solener.2017.10.050)
- [25] A. Hassan, A. Wahab, M. A. Qasim, M. M. Janjua, M. A. Ali, H. M. Ali, T. R. Jadoon, E. Ali, A. Raza, N. Javaid, Thermal management and uniform temperature regulation of photovoltaic modules using hybrid phase change materials-nanofluids system, *Renewable Energy*, 145. DOI: [10.1016/j.renene.2019.05.130](https://doi.org/10.1016/j.renene.2019.05.130)
- [26] H. G. Teo, P. S. Lee, M. N. A. Hawlader, An active cooling system for photovoltaic modules, *Applied Energy*, 90(1). DOI: [10.1016/j.apenergy.2011.01.017](https://doi.org/10.1016/j.apenergy.2011.01.017)
- [27] R. Mazón-Hernández, J. R. García-Cascales, F. Vera-García, A. S. Káiser, B. Zamora, Improving the electrical parameters of a photovoltaic panel by means of an induced or forced air stream, *Int. Journal of Photoenergy*, 2013. DOI: [10.1155/2013/830968](https://doi.org/10.1155/2013/830968)
- [28] K. A. Moharram, M. S. Abd-Elhady, H. A. Kandil, H. El-Sherif, Enhancing the performance of photovoltaic panels by water cooling, *Ain Shams Engineering Journal*, 4(4). DOI: [10.1016/j.asej.2013.03.005](https://doi.org/10.1016/j.asej.2013.03.005)
- [29] S. Dubey, G. N. Tiwari, Thermal modeling of a combined system of photovoltaic thermal (PV/T) solar water heater, *Solar Energy*, 82(7). DOI: [10.1016/j.solener.2008.02.005](https://doi.org/10.1016/j.solener.2008.02.005)
- [30] S. A. Kalogirou, Y. Tripanagnostopoulos, Hybrid PV/T solar systems for domestic hot water and electricity production, *Energy Conversion and Management*, 47(18–19). DOI: [10.1016/j.enconman.2006.01.012](https://doi.org/10.1016/j.enconman.2006.01.012)
- [31] S. Ntsaluba, B. Zhu, X. Xia, Optimal flow control of a forced circulation solar water heating system with energy storage units and connecting pipes, *Renewable Energy*, 89. DOI: [10.1016/j.renene.2015.11.047](https://doi.org/10.1016/j.renene.2015.11.047)
- [32] L. Zhu, R. F. Boehm, Y. Wang, C. Halford, Y. Sun, Water immersion cooling of PV cells in a high concentration system, *Solar Energy Materials and Solar Cells*, 95(2). DOI: [10.1016/j.solmat.2010.08.037](https://doi.org/10.1016/j.solmat.2010.08.037)
- [33] S. Mehrotra, P. Rawat, M. Debbarma, K. Sudhakar, Performance of a solar panel with water immersion cooling technique, *Int. Journal Sci Environ Technol*, 3(3), 2014, pp. 1161-1172.
- [34] M. Rosa-Clot, P. Rosa-Clot, G. M. Tina, P. F. Scandura, Submerged photovoltaic solar panel: SP2, *Renewable Energy*, 35(8). DOI: [10.1016/j.renene.2009.10.023](https://doi.org/10.1016/j.renene.2009.10.023)
- [35] P. Bevilacqua, S. Perrella, D. Cirone, R. Bruno, N. Arcuri, Efficiency improvement of photovoltaic modules via back surface cooling, *Energies*, 14(4). DOI: [10.3390/en14040895](https://doi.org/10.3390/en14040895)
- [36] S. Nizetić, D. Čoko, A. Yadav, F. Grubišić-Čabo, Water spray cooling technique applied on a photovoltaic panel: The performance response, *Energy Conversion and Management*, 108. DOI: [10.1016/j.enconman.2015.10.079](https://doi.org/10.1016/j.enconman.2015.10.079)
- [37] L. H. Yang, J. de Liang, C. Y. Hsu, T. H. Yang, S. L. Chen, Enhanced efficiency of photovoltaic panels by integrating a spray cooling system with shallow geothermal energy heat exchanger, *Renewable Energy*, 134. DOI: [10.1016/j.renene.2018.11.089](https://doi.org/10.1016/j.renene.2018.11.089)
- [38] P. Bevilacqua, R. Bruno, N. Arcuri, Comparing the performances of different cooling strategies to increase photovoltaic electric performance in different meteorological conditions, *Energy*, 195. DOI: [10.1016/j.energy.2020.116950](https://doi.org/10.1016/j.energy.2020.116950)
- [39] P. Bevilacqua, R. Bruno, A. Rollo, V. Ferraro, N. Arcuri, A Novel Thermal Model for PV Panels with Back Surface Spray Cooling, *SSRN Electronic Journal*. DOI: [10.2139/ssrn.3966211](https://doi.org/10.2139/ssrn.3966211)
- [40] F. Nicoletti, M. A. Cucumo, V. Ferraro, D. Kaliakatsos, A. Gigliotti, A Thermal Model to Estimate PV Electrical Power and Temperature Profile along Panel Thickness, *Energies* 2022, 15, 7577. DOI: [10.3390/en15207577](https://doi.org/10.3390/en15207577)
- [41] M. D. Siegel, S. A. Klein, W. A. Beckman, A simplified method for estimating the monthly-average performance of photovoltaic systems, *Solar Energy*, 26(5). DOI: [10.1016/0038-092X\(81\)90220-6](https://doi.org/10.1016/0038-092X(81)90220-6)
- [42] Italian standard UNI 10349 – Heating and cooling of buildings – Climatic data, Italia: UNI, 2016.
- [43] K. Whitfield, C. R. Osterwald, Procedure for determining the uncertainty of photovoltaic module outdoor electrical performance, *Progress in Photovoltaics: Research and Applications*, 9(2). DOI: [10.1002/ppp.356](https://doi.org/10.1002/ppp.356)
- [44] A. Manasrah, M. Masoud, Y. Jaradat, P. Bevilacqua, Investigation of a Real-Time Dynamic Model for a PV Cooling System, *Energies*, 15(5). DOI: [10.3390/en15051836](https://doi.org/10.3390/en15051836)
- [45] M. Cucumo, A. de Rosa, V. Ferraro, D. Kaliakatsos, V. Marinelli, Correlations of direct solar luminous efficacy for all sky, clear sky and intermediate sky conditions and comparisons with experimental data of five localities, *Renewable Energy*, 35(10). DOI: [10.1016/j.renene.2010.04.004](https://doi.org/10.1016/j.renene.2010.04.004)
- [46] A. De Rosa, V. Ferraro, D. Kaliakatsos, V. Marinelli, Calculating diffuse illuminance on vertical surfaces in different sky conditions, *Energy*, 33(11). DOI: [10.1016/j.energy.2008.05.009](https://doi.org/10.1016/j.energy.2008.05.009)